

DISTRIBUTION OF GASEOUS $^{12}\text{CO}_2$, $^{13}\text{CO}_2$, AND $^{14}\text{CO}_2$ IN THE
SUB-SOIL UNSATURATED ZONE OF THE WESTERN US GREAT PLAINS

DC THORSTENSON*, EP WEEKS**, HERBERT HAAS†, and DW FISHER*

ABSTRACT. Data on the depth distribution of the major atmospheric gases and the abundance of gaseous $^{12}\text{CO}_2$, $^{13}\text{CO}_2$, and $^{14}\text{CO}_2$ in the subsoil unsaturated zone have been obtained from several sites in the western Great Plains of the United States. Sample profiles range from land surface to depths of 50m. Although each site must be considered on an individual basis, several general statements can be made regarding the profiles. 1) Diffusion of these gaseous molecules through the unsaturated zone is an important transport mechanism. 2) As predicted by diffusion theory, depth profiles of the various isotopic species of CO_2 differ substantially from one another, depending on individual sources and sinks such as root respiration and oxidation of organic carbon at depth. 3) In general, post-bomb (> 100% modern) ^{14}C activities are not observed in the deep unsaturated zone, in contrast to diffusion model predictions. 4) In spite of generally decreasing ^{14}C activities with depth, absolute partial pressures of $^{14}\text{CO}_2$ in the subsoil unsaturated zone are 1-2 orders of magnitude higher than the partial pressure of $^{14}\text{CO}_2$ in the atmosphere.

INTRODUCTION

JL Kunkler (1969) performed the first ^{14}C analyses of CO_2 gas from the deep unsaturated zone in the Bandelier Tuff at the Los Alamos National Laboratory. His data showed ^{14}C activities > 100% modern carbon (pmc) at depths of 24m and 86m, indicating that post-bomb CO_2 had penetrated the tuff to at least that depth. Kunkler's research remained unique until recent studies on the unsaturated zone by Reardon, Allison, and Fritz (1979) and Reardon, Mozeto, and Fritz (1980). Data are presented here on the abundance and distribution of unsaturated-zone $^{12}\text{CO}_2$, $^{13}\text{CO}_2$, and $^{14}\text{CO}_2$ from several sampling sites in North Dakota and Texas.

* US Geological Survey, Reston, Virginia 22092

** US Geological Survey, Denver, Colorado 80225

† Southern Methodist University, Dallas, Texas 75275

Three of the North Dakota sites were sampled repetitively over a five-year period; two of these sites are discussed in a preliminary attempt to evaluate the role of gaseous diffusion in unsaturated zone processes at these locales. All of the unsaturated zone CO_2 data collected to date by the authors are presented. Although site-specific process models have not been formulated for each site, some important geochemical generalizations can be made.

PHYSICO-CHEMICAL PRINCIPLES

For chemical modeling and equilibrium calculations involving gases, the gas partial pressure is the most useful variable. Alternatively, transport modeling and calculation of diffusive fluxes from Fick's laws require the abundance of diffusing species to be expressed in units of mass/volume (generally $\text{mol}\cdot\text{cm}^{-3}$). These statements hold for any isotopic species of the same gas, as well as for different gases, eg, $^{14}\text{CO}_2$ will diffuse in response to its own concentration gradient regardless of the distribution of $^{12}\text{CO}_2$ and $^{13}\text{CO}_2$ in the gas mixtures*. Outlined below are the methods for calculating partial pressures and concentrations from the original analytical data. For purposes of this paper, the behavior of all gases can be assumed to be ideal.

MAJOR GASES. The analytical data for the unsaturated zone gases are available as volume percent for N_2 , O_2 , Ar, and CO_2 ** , as $\delta^{13}\text{C}(\text{‰})$ for $^{13}\text{CO}_2$, and as $A^{14}\text{C}$ in percent modern carbon (pmc) for $^{14}\text{CO}_2$. Dissolved CO_2 is initially reported as partial pressure. For N_2 , O_2 , Ar, and CO_2 the volume percent equals mol percent, and the mol fraction of a given gas, X_i , is simply $X_i = (\text{vol}\%_i/100)$.

* The fact that different isotopes of a single chemical species must respond only to their own concentration gradients is perhaps best visualized through the random-walk model for diffusive processes (Feynman, Leighton, and Sands, 1963, Chap 43). The independence of isotopic diffusion is the basis for tracer diffusion experiments and is implicit in the general equations for calculating the self-diffusion coefficients of one isotopic species in another (Bird, Stewart, and Lightfoot, 1960; Jost, 1960; Li and Gregory, 1974).

** For simplicity, we use CO_2 to refer to $^{12}\text{CO}_2 + ^{13}\text{CO}_2 + ^{14}\text{CO}_2$ (there is no isotopic separation in the gas chromatograph columns).

The partial pressure of i is given by

$$P_i = X_i P_{\text{total}}^\dagger. \quad (1)$$

Then, from the ideal gas law $n_i/V = P_i/RT$,

$$C_i (\text{mol-cm}^{-3}) \equiv \frac{n_i (\text{mol})}{V (\text{cm}^3)} = \frac{X_i P_{\text{total}} (\text{atm})}{R (\text{cm}^3\text{-atm-K}^{-1}\text{-mol}^{-1}) T (\text{K})}. \quad (2)$$

^{13}C . The molar ratio, R , of $^{13}\text{CO}_2$ to CO_2 in the PDB standard ($\delta^{13}\text{C} \equiv 0$) is 0.0111 (Landgren, 1954). Given this value, concentrations of $^{13}\text{CO}_2$ can be calculated from $\delta^{13}\text{C}$ values and total CO_2 concentrations as follows:

$$\delta^{13}\text{C} \equiv \left\{ \frac{R_{\text{sample}}}{R_{\text{reference}}} - 1 \right\} 1000 = \left\{ \frac{R_{\text{sample}}}{0.0111} - 1 \right\} 1000. \quad (3)$$

Rearranging,

$$R_{\text{sample}} = \frac{C(^{13}\text{CO}_2)}{C(\text{CO}_2)} = 0.0111 \{ 1 + (\delta^{13}\text{C}/1000) \}, \quad (4)$$

and

$$C(^{13}\text{CO}_2) = [C(\text{CO}_2)](0.0111) \{ 1 + (\delta^{13}\text{C}/1000) \}. \quad (5)$$

The relative gradients of $^{13}\text{CO}_2$ and CO_2 will therefore differ only by the factor $(1 + \delta^{13}\text{C}/1000)$. Total variation of this factor through the range of $\delta^{13}\text{C}$ values observed in this study amounts to < 2%, which is of about the same magnitude as the uncertainty in CO_2 collection and analysis. Therefore, transport modeling of $^{13}\text{CO}_2$ will produce results essentially identical to those for CO_2 , with calculated fluxes multiplied by 0.0111. The utility of the ^{13}C signature as a means of identifying sources of carbon in the system remains undiminished, although the ^{13}C variations are not emphasized in this report.

† For the North Dakota sites, $P_{\text{total}} = 0.91$ atm; at the Texas sites $P_{\text{total}} = 0.88$ atm; and at Los Alamos, $P_{\text{total}} = 0.77$ atm

^{14}C . For ^{14}C , the ratio $R_{^{14}\text{CO}_2} = (\text{moles } ^{14}\text{CO}_2)/(\text{moles } \text{CO}_2)$ must be obtained from analytical values of $A^{14}\text{C}(\text{pmc})^*$. The quantity $R_{^{14}\text{CO}_2}$ can be obtained from the decay equation $-dN/dt = \lambda N$ where N is the number of ^{14}C atoms per gram of carbon, and the decay constant λ has the value $3.84 \times 10^{-12} \text{ sec}^{-1}$.

For a 100 pmc sample, the decay rate is 0.226 dps/g-C. In this case

$$N = \frac{-dN/dt}{\lambda} = \frac{0.226}{3.84 \times 10^{-12}} = 5.89 \times 10^{10} \text{ atoms } ^{14}\text{C/g-C}, \quad (6)$$

or, introducing Avogadro's number and the atomic weight of carbon,

$$R_{^{14}\text{CO}_2} = \frac{5.89 \times 10^{10} / 6.023 \times 10^{23}}{1 / 12.011} = 1.17 \times 10^{-12} \frac{\text{mol } ^{14}\text{C}}{\text{mol C}} \text{ at } 100\text{pmc}. \quad (7)$$

Then for a 1 pmc sample, $R_{^{14}\text{CO}_2}$ would be $1.17 \times 10^{-14} \text{ mol } ^{14}\text{C}$ per mol C, and for an arbitrary ^{14}C activity

$$R_{^{14}\text{CO}_2} = (1.17 \times 10^{-14}) (A^{14}\text{C}(\text{pmc})) \text{ mol } ^{14}\text{C/mol C}. \quad (8)$$

The mole fraction of $^{14}\text{CO}_2$ in the original gas sample is then

$$X_{^{14}\text{CO}_2} = (R_{^{14}\text{CO}_2})(X_{\text{CO}_2}) = (1.17 \times 10^{-16}) (A^{14}\text{C}(\text{pmc}))(\text{vol\% } \text{CO}_2). \quad (9)$$

* Reardon, Mozeto, and Fritz (1980) discussed the distribution of $^{14}\text{CO}_2$ in the unsaturated zone as a function of $R_{^{14}\text{CO}_2}$. Their conclusions will be correct to the extent that the CO_2 content of the gas phase is constant.

Partial pressures will be given by

$$P_{^{14}\text{CO}_2} = X_{^{14}\text{CO}_2} P_{\text{total}} \quad (10)$$

Concentrations of $^{14}\text{CO}_2$ will be given by combining equations (2) and (9), with $R = 82.05 \text{ atm-cm}^3\text{-mol}^{-1}\text{-K}^{-1}$:

$$C_{^{14}\text{CO}_2} = \frac{X_{^{14}\text{CO}_2} P_{\text{total}}}{RT} = \quad (11)$$

$$= \frac{(1.43 \times 10^{-18})(A^{14}\text{C}(\text{pmc}))(\text{Vol}\% \text{CO}_2)(P_{\text{total}}(\text{atm}))}{T(\text{K})} \text{ in } \frac{\text{mol}^{14}\text{CO}_2}{\text{cm}^3}$$

The values of $A^{14}\text{C}(\text{pmc})$ to be used in equation (11) must be uncorrected because no age estimation is intended, and the chemical parameters of interest require only raw data on the isotopic abundances.

DIFFUSION MODELING

As mentioned above, each isotopic species of CO_2 within the soil gas diffuses through the unsaturated zone according to its own concentration gradient as described by Fick's Second Law. However, for movement in the unsaturated zone, Fick's Second Law must be modified to account for the effects of the porous medium structure on the rate of diffusion and for reactions between the gas and the liquid and solid phases of the medium. With these modifications, the Law becomes

$$\tau_D^{\theta} \frac{\partial^2 C_A}{\partial x^2} = \theta_D \frac{\partial C_A}{\partial t} + \rho_w (\theta_T - \theta_D) \frac{\partial C_A^+}{\partial t} + \frac{\partial \bar{C}_A}{\partial t} + \alpha_T, \quad (12)$$

where

τ = a tortuosity factor accounting for the added resistance to diffusion imposed by the structure of the porous medium (dimensionless);

- θ_D = drained or gas-filled porosity (dimensionless);
 D_{AB} = molecular diffusion constant for diffusion of gas A into gas B (cm^2/sec);
 C_A = concentration of gas A (mol/cm^3);
 x = dimension increasing with depth; $\equiv 0$ at land surface (cm);
 t = time (sec);
 ρ_w = density of soil water (g/cm^3);
 θ_T = total porosity (dimensionless);
 $\dagger C_A$ = concentration of gas A transferred to the soil water (mol/g of water);
 \bar{C}_A = concentration of substance A transferred to the solid phase ($\text{mol}/[\text{cm}^3$ of medium], where $[\text{cm}^3$ of medium] refers to the space occupied by solids + liquids + gases);
 and α_T = a production term for substance A [$\text{mol}/(\text{cm}^3$ of medium)/sec].

Equation (12) states that the rate of one-dimensional diffusion of gas A toward a given point minus the rate of diffusion from the point is equal to the combined rate of change in concentration in 1) the gas phase, 2) the liquid phase, as dissolved gas and any dissolved chemical species containing the gas molecule, 3) in the solid phase, plus 4) the amount of the gas produced or consumed at that point per unit time.

THE DIFFUSION COEFFICIENT. The diffusivity of CO_2 in free air has been measured to be $0.144 \text{ cm}^2/\text{sec}$ at STP (Bird, Stewart, and Lightfoot, 1960), which is corrected within the program to ambient conditions by the equation

$$D_{AB} = D_{AB}^{\circ} \left(\frac{P_0}{P} \right) \left(\frac{T}{T_0} \right)^{1.823} *, \quad (13)$$

* Equation (13) is based on Bird, Stewart, and Lightfoot (1960), p 505, eq 16.3-1.

where D_{AB}° = diffusion constant at STP (cm^2/sec);

P_0 = standard atmospheric pressure (one atmosphere);

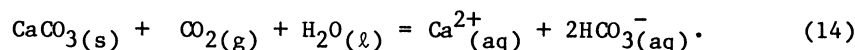
P = mean atmospheric pressure at site (atmospheres);

T = mean annual air temperature at site (K);

and T_0 = temperature at standard conditions (273.2 K).

EVALUATION OF $\partial C_A^\dagger/\partial t$ AND $\partial \bar{C}_A/\partial t$. To evaluate the partitioning of CO_2 between the gas and liquid phase requires a functional relationship between P_{CO_2} and the total dis-

solved CO_2 . A simple function that can be used in the transport program becomes available if the aqueous chemistry in the unsaturated zone can be ascribed to few or one reaction. For this model, it is assumed that calcite is present throughout the unsaturated zone, and that carbonate chemistry in the water is governed by CO_2 - calcite equilibria via reaction (14):



The equilibrium constant for this reaction is

$$K_{\text{eq}} = \frac{a_{\text{Ca}^{2+}} a_{\text{HCO}_3^-}^2}{P_{\text{CO}_2}} \quad , \quad (15)$$

and if this is the only reaction considered,

$$m_{\text{Ca}^{2+}} = \frac{1}{2} m_{\text{HCO}_3^-} \quad . \quad (16)$$

If we assume ideality ($a_i = m_i$),

$$K_{\text{eq}} = \frac{m_{\text{HCO}_3^-}^3}{2 P_{\text{CO}_2}} \quad , \quad (17)$$

or,

$$m_{\text{HCO}_3^-}(\text{aq}) = (2 K_{\text{eq}} P_{\text{CO}_2})^{1/3} = 1.260 K_{\text{eq}}^{1/3} P_{\text{CO}_2}^{1/3}, \quad (18)$$

where

m_i = molality and P_{CO_2} = partial pressure of CO_2 in atm* .

Use of the partitioning coefficient concept to model transport in the gas phase relies on determining the amount of the subject gas going into solution due to a change in concentration in the gas phase. In reaction (14) 1/2 of the aqueous CO_2 comes from solid-phase carbonate dissolution, and the other half by solution from the gas phase. Thus, in equation (12),

$$\frac{\partial \bar{C}_A}{\partial t} = -\frac{1}{2} \rho_w (\Theta_T - \Theta_D) \frac{\partial C_A^\dagger}{\partial t}, \quad (19)$$

where the minus sign indicates that $\text{CaCO}_3(\text{s})$ decreases as $\text{CO}_2(\text{g})$ increases. The relation $\partial C_A^\dagger / \partial t = (\partial C_A^\dagger / \partial C_A)(\partial C_A / \partial t)$, in conjunction with equation (19), allows equation (12) to be expressed only in terms of C_A , as derived below. From equation (18),

$$m_{\text{HCO}_3^-} = (2 K_{\text{eq}} P_{\text{CO}_2})^{1/3}. \quad (20)$$

However, the concentration in mol/cm^3 is essentially equal to $m_{\text{HCO}_3^-}/1000$. Thus,

$$C_A^\dagger = 10^{-3} (2 K_{\text{eq}} P_{\text{CO}_2})^{1/3}. \quad (21)$$

To express all terms as a function of C_A , rather than P_{CO_2} , the gas law is employed as in equation (2):

* This model is a simplified version of the calculation of carbonate equilibria at a given P_{CO_2} (see, eg, Garrels and Christ, 1965, p 81-83).

$$C_A = \frac{n}{V} = \frac{P_{\text{CO}_2}}{RT},$$

or
$$P_{\text{CO}_2} = RT C_A.$$

With P in atm, C_A in mol/cm³, and T in kelvins, $R = 82.05$ atm-cm³-mol⁻¹-K⁻¹. Therefore

$$C_A^\dagger = 10^{-3} (2K_{\text{eq}})^{1/3} (82.05TC_A)^{1/3}, \quad (22)$$

$$C_A^\dagger = 5.475 \times 10^{-3} (K_{\text{eq}}T)^{1/3} C_A^{1/3}, \quad (23)$$

and thus

$$\frac{\partial C_A^\dagger}{\partial C_A} = 1.825 \times 10^{-3} (K_{\text{eq}}T)^{1/3} C_A^{-2/3}. \quad (24)$$

Combining equations (24) and (19), expressing the fact that only 1/2 of the change in C_A^\dagger is due to CO_2 from the gas phase, equation (12) becomes

$$\begin{aligned} \tau_{\text{D}}^{\text{D}} \frac{\partial^2 C_A}{\partial x^2} &= \\ &= \left\{ \theta_{\text{D}} + 9.125 \times 10^{-4} (\theta_{\text{T}} - \theta_{\text{D}}) (K_{\text{eq}}T)^{1/3} C_A^{-2/3} \right\} \frac{\partial C_A}{\partial t} + \alpha_{\text{T}}. \end{aligned} \quad (25)$$

The same equation can be expressed in terms of P_{CO_2} by substituting P_{CO_2}/RT for C_A (from the gas law) in equation (25) and multiplying by RT to give

$$\tau_{\theta_D} D_{AB} \frac{\partial^2 P_{CO_2}}{\partial x^2} = \quad (26)$$

$$= \left\{ \theta_D + 9.125 \times 10^{-4} (\theta_T - \theta_D) (K_{eq} T)^{1/3} [P_{CO_2}/RT]^{-2/3} \right\} \frac{\partial P_{CO_2}}{\partial t} + RT \alpha_T,$$

or

$$\tau_{\theta_D} D_{AB} \frac{\partial^2 P_{CO_2}}{\partial x^2} = \quad (27)$$

$$= \left\{ \theta_D + 0.01723 T (\theta_T - \theta_D) K_{eq}^{1/3} P_{CO_2}^{-2/3} \right\} \frac{\partial P_{CO_2}}{\partial t} + 82.05 T \alpha_T.$$

Either equation (25) or equation (27) may be used for modeling purposes, depending on convenience or preference.

THE PRODUCTION TERM. The high concentration of CO_2 in the unsaturated zone relative to that in the atmosphere results from root respiration, microbial activity, and oxidation of organic carbon in the soil zone. All of these activities usually occur mainly near the surface, and in our model were assumed to occur uniformly with depth from land surface to a depth of 1m, but not to occur below that depth. Attempts to include additional CO_2 production at greater depths (see Site 4, fig 6) have not yet been made.

CO_2 production is seasonal, however, with annual production approximately constant, resulting in an essentially steady CO_2 partial pressure at depth. Both average and seasonal production rates were used in our modeling exercises. The average production rate was determined using an equation developed by van Bavel (1951), based on the root-zone production profile described above, a constant partial pressure of CO_2 in the atmosphere at land surface, and no diffusion of CO_2 across the water table. His equation is

$$\frac{\alpha}{a^2} = \frac{2 \theta_D \tau D_{AB} (C_{depth} - C_{atm})}{a^2}, \quad (28)$$

where $\bar{\alpha}$ = the average production rate of CO_2 in the root zone (mol/cm^3 of medium/sec);

C_{depth} = CO_2 concentration at depth (mol/cm^3);

C_{atm} = CO_2 concentration in the atmosphere (mol/cm^3);

a = depth of root zone (cm);

and other symbols are defined above.

To model seasonal variations in P_{CO_2} with depth, it is assumed that the CO_2 production rate in the root zone is proportional to that given by a sine curve during the growing season, and that the rate is zero during the rest of the year. The amplitude of the production curve is calculated to provide the same total production for the year as that determined from the average production rate. Based on integration of the area under the sine curve, this amplitude is

$$\Omega = \frac{\pi}{2} (T_{\text{tot}}/T_{\text{P}}) \bar{\alpha} \quad , \quad (29)$$

where

Ω = the maximum rate of CO_2 production, (mol/cm^3 of medium/sec);

T_{tot} = total time (one year);

T_{P} = time of CO_2 production (in fraction of a year);

and other symbols are as defined above. Thus, the seasonal production rate may be expressed in equation form

$$\alpha_T = \frac{\pi T_{\text{tot}}}{2 T_{\text{P}}} \sin\left[\frac{\pi (T - T_0)}{T_{\text{P}}}\right] \quad , \quad T_0 \leq T \leq (T_0 + T_{\text{P}}); \quad (30)$$

and

$$\alpha_T = 0, \quad T < T_0 \quad \text{or} \quad T > (T_0 + T_{\text{P}}); \quad (31)$$

where

α_T = production rate at time T (mol/cm^3 of medium/sec);

T = time (years);

T_0 = time at which seasonal production starts (years).

DATA PRESENTATION

Table 1 presents the various derived parameters P_{CO_2} , X_{CO_2} , and P_{14CO_2} for all samples collected. The more standard $\delta^{13}C$ and $A^{14}C$ data are provided for comparison. P_{13CO_2} was not tabulated because for all practical purposes $P_{13CO_2} \cong 10^{-2}P_{CO_2}$. Table 2 includes additional compositional data for the principal atmospheric gases. Seasonal variations of P_{CO_2} in individual probes are shown in figure 1, seasonal variation of P_{14CO_2} in figure 4, and depth profiles of P_{CO_2} and P_{14CO_2} in figure 6.

MODEL APPLICATION

Only two sites provide sufficient data to attempt seasonal modeling (North Dakota Sites 4 and 6); only Site 6 contains calcite throughout the unsaturated zone. The modeling efforts presented here are thus limited to North Dakota Site 6. The location and hydrogeologic characteristics of this site are described in Haas et al (1983). Models are presented first for the time and depth distribution of CO_2 , then for the time and depth distribution of $^{14}CO_2$.

CO_2 concentrations in the unsaturated zone were modeled for this study using a numerical solution to the finite-difference form of equation (27), as described by Weeks, Earp, and Thompson (1982). Briefly, for modeling purposes, the entire unsaturated zone is divided into equal nodal increments, and a finite-difference equation is written for each node. Variations in media properties are accounted for

TABLE 1. Carbon dioxide and carbon isotopes at various depths from sites in southwestern North Dakota, west Texas, and New Mexico

Date of collection	Vol % CO_2	P_{CO_2} atm x 10 ²	$\delta^{13}\text{CO}_2$ ‰	X_{14}CO_2 x 10 ¹⁴	P_{14}CO_2 atm x 10 ¹⁴	C_{14}CO_2 x 10 ²⁰	Vol % CO_2	P_{CO_2} atm x 10 ²	$\delta^{13}\text{CO}_2$ ‰	X_{14}CO_2 pmc	A^{14}CO_2 pmc	X_{14}CO_2 x 10 ¹⁴	P_{14}CO_2 atm x 10 ¹⁴	C_{14}CO_2 x 10 ²⁰
Site 6, ND														
Water table = 14.5m														
South 4" well (15.9m) b/														
6/30/81	0.033	0.030	-8.1	125.99	0.049	1.91	2.3	0.46	-6.8	17.29	17.29	-	0.47 b/	-
10/07/81	0.033	0.030	-7.8	129.05	0.050	1.96	2.2	0.48	-7.3	18.84	18.84	-	0.48	-
North 4" well (17.4m) b/														
8/10/80	-	-	-23.5	118.08	-	-	2.4	0.46	-5.3	21.24	21.24	b/	0.60 b/	b/
12/04/80	-	-	-18.3	103.62	-	-	1.9	0.47	-6.7	20.53	20.53	-	0.50	-
3/04/81	-	-	-18.1	99.07	-	-	2.1	0.49	-6.2	20.10	20.10	-	0.51	-
6/25/81	-	-	-24.6	122.67	-	-	2.2	0.50	-6.4	19.99	19.99	-	0.51	-
10/06/81	-	-	-24.0	124.83	-	-	2.2	0.51	-6.4	20.41	20.41	-	0.53	-
Site 4, ND														
Surface a/														
7/06/77	1.63	1.48	-	-	-	-	-	-	-	-	-	-	-	-
8/23/78(8b)	2.3	2.20	-	-	-	-	-	-	-	-	-	-	-	-
5/22/79	1.08	0.98	-24.2	114.13	1.44	56.7	0.46	0.40	-27.9	103.00	103.00	0.53	0.48	20.8
8/10/80(8a)	2.00	1.82	-22.6	113.26	2.65	104.2	0.92	0.84	-20.3	95.13	95.13	1.02	0.50	20.3
12/04/80	1.48	1.35	-22.6	112.79	1.95	76.8	0.56	0.51	-20.8	83.72	83.72	0.55	0.50	21.0
3/04/81	0.98	0.89	-22.5	112.18	1.29	50.6	0.40	0.36	-21.5	81.52	81.52	0.38	0.35	15.0
6/25/81	1.28	1.16	-22.5	112.52	1.68	66.3	0.71	0.65	-20.8	87.38	87.38	0.73	0.66	28.5
10/06/81	1.79	1.65	-22.5	112.33	2.35	92.5	1.09	0.99	-21.3	91.70	91.70	1.17	1.06	46.0
Probe 1 (2.7a)														
5/23/79 (6b)	0.73	0.73	-	-	-	-	-	-	-	-	-	-	-	-
8/16/80(8a)	0.92	0.84	-	-	-	-	-	-	-	-	-	-	-	-
12/05/80	0.56	0.51	-	-	-	-	-	-	-	-	-	-	-	-
3/05/81	0.40	0.40	-	-	-	-	-	-	-	-	-	-	-	-
6/26/81(6a)	0.71	0.65	-	-	-	-	-	-	-	-	-	-	-	-
10/05/81	1.09	0.99	-	-	-	-	-	-	-	-	-	-	-	-
Probe 2 (5.8a)														
5/23/79 (6b)	1.32	1.20	-	-	-	-	-	-	-	-	-	-	-	-
8/23/78(8b)	4.90	4.46	-	-	-	-	-	-	-	-	-	-	-	-
5/23/79	5.63	5.12	-27.9	-	-	-	-	-	-27.9	10.00	10.00	0.66	0.60	25.9
8/16/80(8a)	5.34	4.86	-	-	-	-	-	-	-	10.92	10.92	0.68	0.62	26.8
12/05/80	6.69	6.09	-22.2	-	-	-	-	-	-22.2	8.79	8.79	0.69	0.62	27.0
6/25/81	4.63	4.21	-23.3	-	-	-	-	-	-23.3	8.82	8.82	0.48	0.43	18.8
10/05/81	5.55	5.03	-21.9	-	-	-	-	-	-21.9	9.29	9.29	0.51	0.46	19.9
Probe 3 (9.1a)														
6/25/77(6b)	17.8	16.2	-	-	-	-	-	-	-	2.4	2.4	-50	0.45	19.6
8/23/78(8b)	18.0	16.4	-	-	-	-	-	-	-	-	-	-	-	-
5/23/79	15.7	14.3	-29.4	-	-	-	-	-	-29.4	1.75	1.75	0.32	0.29	12.6
3/16/80(8a)	18.9	17.1	-24.0	-	-	-	-	-	-24.0	1.43	1.43	0.31	0.29	12.4
10/05/80	17.0	16.1	-24.0	-	-	-	-	-	-24.0	2.35	2.35	0.44	0.44	19.1
3/05/81	17.0	16.2	-23.7	-	-	-	-	-	-23.7	2.72	2.72	0.34	0.49	21.3
6/26/81(6a)	18.3	16.7	-23.7	-	-	-	-	-	-23.7	4.46	4.46	0.44	0.44	18.7
10/05/81	18.9	17.2	-23.2	-	-	-	-	-	-23.2	1.81	1.81	0.40	0.36	15.7

(Table 1 cont'd)

Date of collection	Vol. % CO ₂	P _{CO₂} atm x 10 ²	δ ¹³ O ₂ ‰	A ¹⁴ O ₂ pmc	X ¹⁴ O ₂ x 10 ¹⁴	P ₁₄ O ₂ atm x 10 ¹⁴	C ₁₄ O ₂ x 10 ²⁰	Date of collection	Vol. % CO ₂	P _{CO₂} atm x 10 ²	δ ¹³ O ₂ ‰	A ¹⁴ O ₂ pmc	X ¹⁴ O ₂ x 10 ¹⁴	P ₁₄ O ₂ atm x 10 ¹⁴	C ₁₄ O ₂ x 10 ²⁰	
Site 4 (continued)																
Probe 4 (12.8m)																
6/29/77 (6b)	16.6	15.1	-	-	-	-	-	9/10/76	18.9	17.2	-	-	-	-	-	
8/23/78 (8b)	18.0	16.4	-	-	-	-	-	6/28/77	13.2	12.0	-17.28	2.1	0.32	0.30	12.8	
5/23/79	16.8	15.3	-	2.09	.41	0.37	16.1	8/13/80	1.59	1.45	-16.6	20.35	0.38	0.34	14.9	
8/16/80 (8a)	18.6	16.9	-24.1	2.38	.47	0.43	18.6	12/06/80	8.17	7.16	-15.4	3.04	0.33	0.32	13.9	
3/05/80	17.0	15.5	-23.8	2.82	.56	0.51	22.0	6/28/81	5.49	4.09	-16.4	3.12	0.20	0.18	7.9	
6/26/81 (8a)	18.3	16.7	-23.1	-	-	-	-	10/08/81	1.33	1.21	-16.0	-	-	-	-	
10/05/81	18.7	17.0	-23.9	2.40	.53	0.48	20.6	Water table ± 14.0m								
4" well (16.5m) b/																
3/05/80	-	9.0	-17.1	6.73	b/	0.71	b/	9/02/80	-	6.0	-	-	-	-	-	b/
3/05/80	-	8.1	-16.7	6.51	-	0.62	-	9/02/81	-	6.3	-	-	-	-	-	-
6/26/81	-	8.1	-16.8	6.26	-	0.59	-	10/05/81	-	5.9	-11.7	37.98	-	2.62	-	-
10/05/81	-	8.3	-16.6	5.89	-	0.57	-	Site 2, ND								
Probe 1 (2.7m)																
9/10/76	0.056	0.051	-	-	-	-	-	9/13/76	5.42	4.93	-	-	-	-	-	-
6/28/77	0.080	0.073	-	-	-	-	-	6/28/77	6.51	5.92	-21.64	-	-	-	-	-
9/13/80	11.3	10.3	-34.8 (small isotope sample)	-	-	-	-	Probe 2 (5.8m)								
6/28/81	10.4	9.46	-18.1	3.21	0.50	.46	19.8	9/13/76	5.81	5.28	-21.63	18.1	1.67	1.52	65.8	
10/08/81	7.71	7.01	-17.9	5.46	0.49	0.45	19.3	6/28/77	7.93	7.22	-	-	-	-	-	
Probe 2 (5.2m)																
9/10/76	0.56	0.51	-	-	-	-	-	9/13/76	11.3	10.3	-	-	-	-	-	-
6/28/77	1.01	0.98	-	-	-	-	-	9/10/80	11.6	10.5	-	-	-	-	-	-
10/08/81	6.10	5.55	-17.5	6.03	0.43	0.39	16.9	Site 3, ND								
Probe 3 (7.6m) d/																
9/10/76	16.4	14.9	-17.68	2.1	0.65	.61	17.9	9/13/76	11.2	10.2	-12.01	20.6	2.94	2.68	116.	
6/28/77	17.5	16.9	-17.0	1.85	0.37	0.34	14.6	6/28/77	23.2	22.9	-	-	-	-	-	
12/06/80	14.8	13.5	-18.9	1.81	0.31	0.29	12.3	7/03/77	19.4	17.7	-11.68	12.2	2.77	2.52	109.	
3/06/81	15.9	14.5	-17.5	2.06	0.38	0.35	15.1	Probe 3 (6.1m)								
6/28/81	14.4	13.1	-17.6	1.57	0.26	0.24	10.4	9/13/76	24.2	22.0	-	-	-	-	-	
10/08/81	12.3	11.2	-17.5	1.45	0.21	0.19	8.2	7/03/77	19.2	17.5	-	-	-	-	-	
Probe 4 (10.9m)																
9/10/76	16.4	14.9	-17.68	2.1	0.65	.61	17.9	Lamb Site 3/								
6/28/77	17.5	16.9	-17.0	1.85	0.37	0.34	14.6	10/23/78	1.89	1.66	-	-	-	-	-	
12/06/80	14.8	13.5	-18.9	1.81	0.31	0.29	12.3	#5 (5.8m)	0.98	0.95	-	-	-	-	-	
3/06/81	15.9	14.5	-17.5	2.06	0.38	0.35	15.1	#4 (11.0m)	1.08	0.95	-	-	-	-	-	
6/28/81	14.4	13.1	-17.6	1.57	0.26	0.24	10.4	#3 (17.1m)	0.09	0.08	-	-	-	-	-	
10/08/81	12.3	11.2	-17.5	1.45	0.21	0.19	8.2	#2 (21.4m)	0.14	0.12	-	-	-	-	-	
								#1 (26.5m)	0.03	0.03	-	-	-	-	-	

(Table 1 cont'd)

Date of collection	Vol % CO ₂	P _{CO₂} atm x 10 ²	δ ¹³ -CO ₂ ‰	A ¹⁴ CO ₂ ‰	X ¹⁴ CO ₂ x 10 ¹⁴	P _{CO₂} atm x 10 ¹⁴	C ¹⁴ CO ₂ x 10 ²⁰
Lamb Site (continued)							
4/17/79							
#5 (3.8b)	2.91	2.65	-20.6	113.1	3.85	3.39	143.
#4 (11.0b)	2.10	1.35	-18.7	108.4	2.27	2.30	99.4
#3 (11.0b)	2.10	1.35	-18.7	108.4	2.27	2.34	99.0
#2 (21.4b)	2.22	1.94	-21.2	108.6	2.82	2.48	106.
Glenn Site^{1/}							
5/79							
#5 (31.4b)	0.57	0.50	-	-	-	-	-
#3 (25.3b)	1.01	0.89	-	-	-	-	-
#2 (36.3b)	0.86	0.76	-	-	-	-	-
#1 (44.5b)	0.06	0.05	-	-	-	-	-
10/79							
#6 (7.0b)	0.36	0.32	-16.03	97.18	0.41	0.36	15.2
#5 (11.0b)	0.68	0.59	-17.3	60.22	0.48	0.44	17.8
#4 (19.8b)	1.13	0.99	-23.1	63.71	0.84	0.74	31.3
#3 (25.3b)	0.59	0.52	-27.7	62.45	0.43	0.38	16.0
#2 (36.3b)	0.98	0.86	-25.9	56.18	0.64	0.57	23.9
Kunkler (1969) ^{1/}							
8/24/67							
TA-52-22	0.47	0.36	-18.5	101	0.56	0.43	18.3
83-0-88.8a							
9/5/67							
TA-52-23	0.89	0.69	-17.9	115	1.20	0.92	39.4
23-8-23.3a							
Reardon et al (1980) ^{1/}							
3-7m	0.4	0.4	- ^{k/}	~ 110	0.51	0.51	22.

Footnotes to Table 1

- a. Calculated from eq (1), with X_{CO₂} = vol % CO₂/100, P_{total} = 0.91, 0.88, and 0.77atm at North Dakota, Texas, and New Mexico sites, respectively.
- b. PDB standard
- c. Calculated from eq (9)
- d. Calculated from eq (10); P_{total} as in footnote a
- e. Calculated from eq (11); " " " " " "
- f. North Dakota = 283K, Texas = 289K, New Mexico = 283K
- g. The inlet for the air sample was 2m above land surface.
- h. Volume % CO₂ (and thus, P_{CO₂}) were not measured in the soil zone. The surface samples represent CO₂ that diffused out of the soil zone.
- i. These analyses represent dissolved gases in shallow groundwater. The values reported for P_{CO₂} represent the partial pressure of dissolved CO₂, P_{CO₂(aq)}. It can be shown that P_{CO₂(aq)} = (R₁₄ / C₁₄) (P_{CO₂(aq)}). Because there is no gas phase present, X₁₄CO₂ and C₁₄CO₂ are not relevant for these samples.
- j. No samples were obtained; periodic attempts produced a vacuum whenever this probe was pumped.
- k. For additional data on CO₂ contents of the Texas sites, see Petratis (1981).
- l. These data (Kunkler, 1969) are from the unsaturated zone in the Bandelier Tuff near Los Alamos, New Mexico.
- m. These data are from the unsaturated zone in a forested area underlain by calcareous sand at Trout Creek, Ontario, Canada. The numbers cited are estimated average values. For further details, see Reardon et al (1979; 1980).

TABLE 2. Nitrogen, argon, and oxygen contents of unsaturated-zone and dissolved gases from sites in southwestern North Dakota and in west Texas

Date of collection	N ₂	Ar	O ₂	Date of collection	N ₂	Ar	O ₂	Date of collection	N ₂	Ar	O ₂
Site 1, ND											
Probe 1 (1.2m)											
7/03/77	75.5	1.0	11.1	7/10/76	96.8	1.3	1.8	7/10/76	81.7	1.1	16.7
7/03/77	77.7	1.0	9.6	6/28/77	78.1	1.0	20.8	6/28/77	89.7	1.9	1.4
Probe 2 (3.4m)											
9/13/76	72.6	1.0	.96	8/13/80	77.1	1.0	10.6	8/13/80	74.9	1.0	12.5
7/03/77	79.7	1.1	.6	3/06/81	80.7	.9	5.0	10/08/81	77	1.0	16.0
Probe 3 (6.1m)											
9/13/76	73.0	1.0	.31	10/08/81	76	1.0	15.0	6/28/77	82.1	1.4	.06
7/03/77	79.0	1.1	.03	6/28/77	80.1	1.1	3	8/13/80	78.6	1.0	3.2
Site 2, ND											
Probe 1 (2.7m)											
6/28/77	83.9	1.0	10.1	6/28/77	80.1	1.1	3	12/06/80	79.0	1.0	5.2
6/28/77	79.2	1.0	13.6	6/28/77	82.1	1.4	.06	3/06/81	79.5	1.0	3.7
Probe 2 (5.8m)											
9/13/76	86.7	1.1	6.2	6/28/81	77.7	1.1	6.9	10/08/81	78	1.1	9.7
6/28/77	79.5	1.1	11.6	6/28/81	78	1.1	9.7	6/28/81	78	1.1	9.7
Probe 3 (8.8m)											
9/13/76	87.0	1.2	.43	10/08/81	76	1.0	20	6/28/81	78	1.1	9.7
9/13/76	87.0	1.2	.15								
Site 3, ND											
Probe 3 (9.1m)											
6/29/77	81.0	1.1	.15	6/28/81	77.7	1.1	6.9	6/28/81	78	1.1	9.7
8/23/78	80.9	1.1	.06	10/08/81	78	1.1	9.7	10/08/81	78	1.1	9.7
5/23/79	81.4	1.1	1.09	6/28/81	77.7	1.1	6.9	6/28/81	78	1.1	9.7
12/05/80	80.8	1.0	.5	6/28/81	77.7	1.1	6.9	6/28/81	78	1.1	9.7
3/05/81	81.7	1.0	.5	6/28/81	77.7	1.1	6.9	6/28/81	78	1.1	9.7
6/26/81	80.7	1.0	<.06	6/28/81	77.7	1.1	6.9	6/28/81	78	1.1	9.7
10/05/81	80	1.0	.34	6/28/81	77.7	1.1	6.9	6/28/81	78	1.1	9.7
Probe 4 (12.8m)											
6/25/78	86.2	1.1	.11	6/28/81	77.7	1.1	6.9	6/28/81	78	1.1	9.7
6/25/78	86.2	1.1	.06	6/28/81	77.7	1.1	6.9	6/28/81	78	1.1	9.7
5/23/79	81.8	1.1	.3	6/28/81	77.7	1.1	6.9	6/28/81	78	1.1	9.7
8/16/80	80.3	1.0	.06	6/28/81	77.7	1.1	6.9	6/28/81	78	1.1	9.7
12/05/80	81.2	1.0	.3	6/28/81	77.7	1.1	6.9	6/28/81	78	1.1	9.7
3/05/81	81.7	.9	.3	6/28/81	77.7	1.1	6.9	6/28/81	78	1.1	9.7
6/26/81	80.8	1.0	<.06	6/28/81	77.7	1.1	6.9	6/28/81	78	1.1	9.7
10/05/81	80	1.1	.35	6/28/81	77.7	1.1	6.9	6/28/81	78	1.1	9.7
4" well (16.5m) Pressure, atmospheres											
8/16/80	.97	.012	<.001	6/28/81	77.7	1.1	6.9	6/28/81	78	1.1	9.7
12/05/80	.94	.011	<.002	6/28/81	77.7	1.1	6.9	6/28/81	78	1.1	9.7
5/05/81	.93	.011	.003	6/28/81	77.7	1.1	6.9	6/28/81	78	1.1	9.7
6/26/81	.98	.011	<.001	6/28/81	77.7	1.1	6.9	6/28/81	78	1.1	9.7
10/05/81	.98	.012	.002	6/28/81	77.7	1.1	6.9	6/28/81	78	1.1	9.7
Site 4, ND											
4" well (17.4m)											
12/04/80	.84	.010	<.001	6/28/81	77.7	1.1	6.9	6/28/81	78	1.1	9.7
3/05/81	.99	.012	.002	6/28/81	77.7	1.1	6.9	6/28/81	78	1.1	9.7
6/25/81	1.16	.012	.012	6/28/81	77.7	1.1	6.9	6/28/81	78	1.1	9.7
10/06/81	1.01	.011	.029	6/28/81	77.7	1.1	6.9	6/28/81	78	1.1	9.7
South 4" well (15.9m) Pressure, atmospheres											
6/23/81	.92	.010	<.001	6/28/81	77.7	1.1	6.9	6/28/81	78	1.1	9.7
10/04/81	.97	.011	.001	6/28/81	77.7	1.1	6.9	6/28/81	78	1.1	9.7
Site 5, ND											
Probe 3 (8.5m)											
7/06/77	79.2	1.0	18.8	6/28/81	77.7	1.1	6.9	6/28/81	78	1.1	9.7
8/23/78	80.4	1.0	17.6	6/28/81	77.7	1.1	6.9	6/28/81	78	1.1	9.7
5/22/79	79.7	1.0	18.2	6/28/81	77.7	1.1	6.9	6/28/81	78	1.1	9.7
3/10/80	78.2	1.0	19.6	6/28/81	77.7	1.1	6.9	6/28/81	78	1.1	9.7
3/04/81	79.2	1.0	18.7	6/28/81	77.7	1.1	6.9	6/28/81	78	1.1	9.7
6/25/81	78.8	1.0	19.0	6/28/81	77.7	1.1	6.9	6/28/81	78	1.1	9.7
10/06/81	79.1	1.0	19	6/28/81	77.7	1.1	6.9	6/28/81	78	1.1	9.7
Site 6, ND											
Probe 1 (2.0m)											
8/1	82.1	1.1	15.2	6/28/81	77.7	1.1	6.9	6/28/81	78	1.1	9.7
8/23/78	77.5	1.0	19.1	6/28/81	77.7	1.1	6.9	6/28/81	78	1.1	9.7
5/22/79	81.3	1.1	16.6	6/28/81	77.7	1.1	6.9	6/28/81	78	1.1	9.7
8/10/80	76.8	1.0	20.2	6/28/81	77.7	1.1	6.9	6/28/81	78	1.1	9.7
12/04/80	77.3	.9	20.3	6/28/81	77.7	1.1	6.9	6/28/81	78	1.1	9.7
3/04/81	78.1	.9	20.0	6/28/81	77.7	1.1	6.9	6/28/81	78	1.1	9.7
6/25/81	78.3	.9	19.5	6/28/81	77.7	1.1	6.9	6/28/81	78	1.1	9.7
10/06/81	78	1.0	19	6/28/81	77.7	1.1	6.9	6/28/81	78	1.1	9.7
Probe 2 (5.8m)											
7/06/77	79.5	1.0	18.1	6/28/81	77.7	1.1	6.9	6/28/81	78	1.1	9.7
8/23/78	78.9	1.0	18.1	6/28/81	77.7	1.1	6.9	6/28/81	78	1.1	9.7
5/22/79	80.2	1.0	17.4	6/28/81	77.7	1.1	6.9	6/28/81	78	1.1	9.7
8/10/80	77.4	1.0	19.9	6/28/81	77.7	1.1	6.9	6/28/81	78	1.1	9.7
12/04/80	77.6	1.0	19.7	6/28/81	77.7	1.1	6.9	6/28/81	78	1.1	9.7
3/04/81	78.6	1.0	19.6	6/28/81	77.7	1.1	6.9	6/28/81	78	1.1	9.7
6/25/81	78.4	1.0	19.0	6/28/81	77.7	1.1	6.9	6/28/81	78	1.1	9.7
10/06/81	78	1.0	19	6/28/81	77.7	1.1	6.9	6/28/81	78	1.1	9.7
Probe 3 (8.5m)											
7/06/77	79.2	1.0	18.8	6/28/81	77.7	1.1	6.9	6/28/81	78	1.1	9.7
8/23/78	80.4	1.0	17.6	6/28/81	77.7	1.1	6.9	6/28/81	78	1.1	9.7
5/22/79	79.7	1.0	18.2	6/28/81	77.7	1.1	6.9	6/28/81	78	1.1	9.7
3/10/80	78.2	1.0	19.6	6/28/81	77.7	1.1	6.9	6/28/81	78	1.1	9.7
3/04/81	79.2	1.0	18.7	6/28/81	77.7	1.1	6.9	6/28/81	78	1.1	9.7
6/25/81	78.8	1.0	19.0	6/28/81	77.7	1.1	6.9	6/28/81	78	1.1	9.7
10/06/81	79.1	1.0	19	6/28/81	77.7	1.1	6.9	6/28/81	78	1.1	9.7
Site 7, ND											
Probe 1 (1.2m)											
7/03/77	75.5	1.0	11.1	6/28/81	77.7	1.1	6.9	6/28/81	78	1.1	9.7
7/03/77	77.7	1.0	9.6	6/28/81	77.7	1.1	6.9	6/28/81	78	1.1	9.7
Probe 2 (3.4m)											
9/13/76	72.6	1.0	.96	6/28/81	77.7	1.1	6.9	6/28/81	78	1.1	9.7
7/03/77	79.7	1.1	.6	6/28/81	77.7	1.1	6.9	6/28/81	78	1.1	9.7
Probe 3 (6.1m)											
9/13/76	73.0	1.0	.31	6/28/81	77.7	1.1	6.9	6/28/81	78	1.1	9.7
7/03/77	79.0	1.1	.03	6/28/81	77.7	1.1	6.9	6/28/81	78	1.1	9.7
Site 8, ND											
Probe 1 (2.7m)											
6/28/77	83.9	1.0	10.1	6/28/81	77.7	1.1	6.9	6/28/81	78	1.1	9.7
6/28/77	79.2	1.0	13.6	6/28/81	77.7	1.1	6.9	6/28/81	78	1.1	9.7
Probe 2 (5.8m)											
9/13/76	86.7	1.1	6.2	6/28/81	77.7	1.1	6.9	6/28/81	78	1.1	9.7
6/28/77	79.5	1.1	11.6	6/28/81	77.7	1.1	6.9	6/28/81	78	1.1	9.7
Probe 3 (8.8m)											
9/13/76	87.0	1.2	.43	6/28/81	77.7	1.1	6.9	6/28/81	78	1.1	9.7
9/13/76	87.0	1.2	.15	6/28/81	77.7	1.1	6.9	6/28/81	78	1.1	9.7

(Table 2 cont'd)

Date of collection	N ₂	Ar	O ₂	Date of collection	N ₂	Ar	O ₂
Lamb site, TX							
10/23/78				4/11/79			
Probe 4	86.6	1.2	11.1	Probe 5	77.8	1.0	20.6
(11.0m)				(13.4m)			
Probe 3	77.6	1.0	20.7	Probe 3	78.4	1.1	19.5
(17.1m)				(25.3m)			
Probe 2	77.3	1.1	20.8	Probe 2	78.6	1.0	19.5
(21.4m)				(36.3m)			
Probe 1	80.9	1.1	17.8	Probe 1	76.8	1.0	22.1
(26.5m)				(44.5m)			
4/79				10/79			
Probe 5	78.8	1.0	17.5	Probe 6	77.7	1.0	21.5
(5.9m)				(7.0m)			
Probe 4	80.5	1.0	16.5	Probe 5	78.1	1.0	20.8
(11.0m)				(13.4m)			
Probe 3	80.5	1.1	15.6	Probe 4	78.9	1.0	19.7
(17.1m)				(19.8m)			
Probe 2	81.1	1.1	15.5	Probe 3	79.1	1.0	20.0
(21.4m)				(25.3m)			
				Probe 2	78.7	1.1	19.4
				(36.3m)			
Glenn site, TX							

by dividing the unsaturated zone into layers, each containing several nodes and within which the properties of the medium, including its tortuosity, drained porosity, and total porosity, are assumed constant. Each screened interval is considered to comprise a layer.

GAS AND MEDIA PROPERTIES. Application of the model requires the input of various parameters to describe the diffusive properties of the gas and medium; the interaction of CO₂ among the gas, liquid, and solid phases within the medium; the production term; boundary conditions at the top and bottom of the unsaturated zone column; and initial conditions at the start of the transient simulation. The values of the parameters used to model North Dakota Site 6 are described below.

Based on observed groundwater temperatures, the mean annual temperature at Gascoyne, North Dakota, is approximated as 10°C. The total pressure is 0.91 atm. The diffusion coefficient of CO₂ in air is calculated internally in the computer program (equation (13)) with these parameters. The equilibrium constant for equation (15) has the value $\log K_{eq}(10^\circ\text{C}) = -5.65^*$. At 283 K, equation (27) thus reduces to

$$\tau_{DAB}^{\theta_D} \frac{\partial^2 P_{CO_2}}{\partial x^2} =$$

$$= \left\{ \theta_D + 0.0638(\theta_T - \theta_D) P_{CO_2}^{-2/3} \right\} \frac{\partial P_{CO_2}}{\partial t} + 2.322 \times 10^4 \alpha_T. \quad (32)$$

The dependence of the rate of mass transfer of CO₂ between the gas and liquid phases upon the gas-phase partial pressure of CO₂ makes equation (32) nonlinear. However, because the value of $P_{CO_2}^{-2/3}$ varies relatively slowly with

P_{CO_2} , no particular problems arise in the numerical solution

of the equation. For this study, $P_{CO_2}^{-2/3}$ for a given time

step was evaluated from the concentration at the previous time step. Small enough time steps (3 days) were used to

* Calculated from the data of Plummer and Busenberg (1982)

ensure that the largest error was $\leq 1\%$, as determined by trial and error.

The materials comprising the unsaturated zone at North Dakota Site 6 include sandy clay from a depth of 0 to 10m, and fine-grained sand below that depth. Based on these textural descriptions, the total porosity was assumed to be 0.35 for the entire profile, as this is a common value for unconsolidated sediments. Drained porosity was assumed to be 0.15 above 10m, and 0.20 below that depth. Tortuosities for the two layers were computed from the relationship (Lai, Tiedje, and Erickson, 1976)

$$\tau = \theta_D^{4/3}, \quad (33)$$

resulting in a value of .08 for the upper layer and of .12 for the lower layer.

THE CO_2 MODEL. Boundary and initial conditions: The concentration of CO_2 at land surface (the upper boundary) is assumed to be specified as a function of time. For the seasonal modeling, P_{CO_2} was assumed constant at .0003 atm,

and the water table, which is at a depth of ca 15m at Site 6, was assumed to be a no-diffusion boundary. Assumed initial conditions are that the partial pressure of CO_2 is 0.014 atm throughout the profile.

Assuming that the average P_{CO_2} at depth is 0.014 atm as measured at 6m at Site 6, that P_{CO_2} in the atmosphere is .0003 atm, and that the root zone depth is 1m, the average rate of production in the root zone at Site 6 is 2.4×10^{-13} mol/cm³ of medium/sec, a value that is calculated internally in the computer program from user-supplied data. The variation of P_{CO_2} with depth is based on a seasonal production rate (equations (29) to (31)) that assumes a five-month growing season that begins on May 1 each year.

RESULTS. The most important influence on CO_2 chemistry in the unsaturated zone at Site 6 appears to be chemical reactions in the soil zone with downward propagation of CO_2 by vapor phase diffusion. The well defined annual cycles of P_{CO_2} at the 3m probe, the attenuation of the cycles with

depth, and the shifts of the maxima and minima to later dates with depth are all consistent with downward diffusion

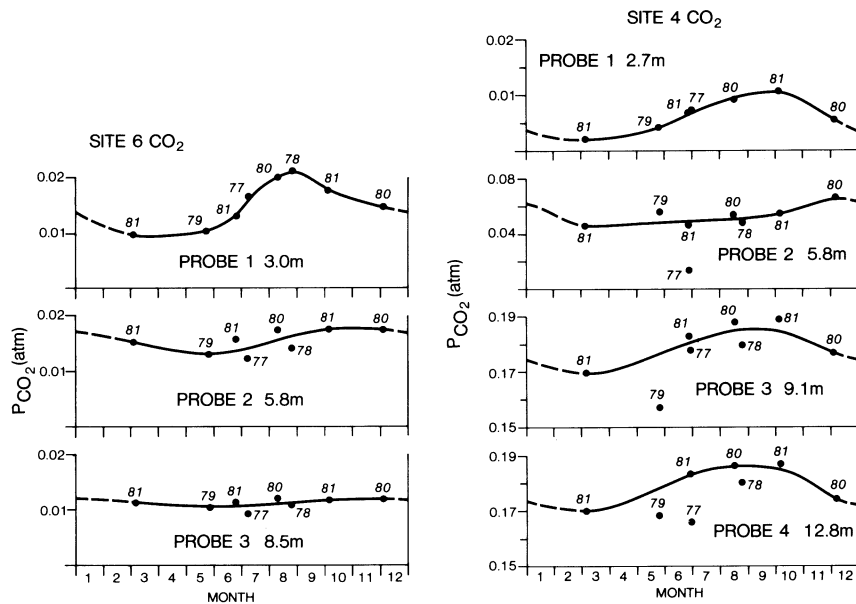


Fig 1. Seasonal variation of P_{CO_2} at North Dakota Sites 6 and 4. Data are plotted by collection date, independent of year, with the year of collection noted at each data point. Data from table 1.

from a seasonally varying source of CO_2 in the soil zone (fig 1). Some details of the modeling results are described below.

Once specific data for Site 6 were incorporated into the mathematical model, the seasonal distribution of P_{CO_2} with

depth was computed, based on the assumption that the CO_2 production history exactly repeats itself every year, an assumption that appears well-justified based on the seasonal cycles in the shallow probes at both Site 6 and Site 4 (fig 1). Five years were simulated to ensure steady cyclic conditions for the final year of simulation. Results, in terms of P_{CO_2} vs depth during each month of the growing season,

are shown in figure 2. These curves are compared (fig 2) with the detailed depth-time CO_2 data from Trout Creek, Ontario (Reardon, Allison, and Fritz, 1979). Qualitative

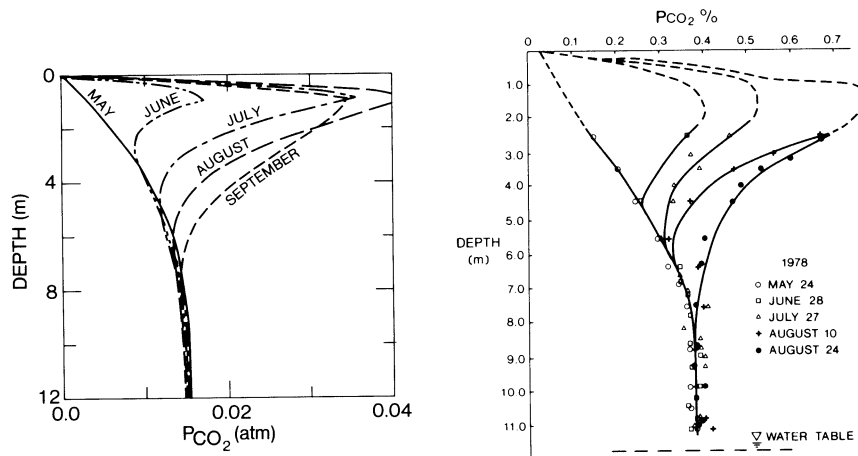


Fig 2. Seasonal profiles of P_{CO_2} vs depth in the unsaturated zone. A. Model calculated for North Dakota Site 6 B. Data from Trout Creek, Ontario; from Reardon, Allison, and Fritz (1979).

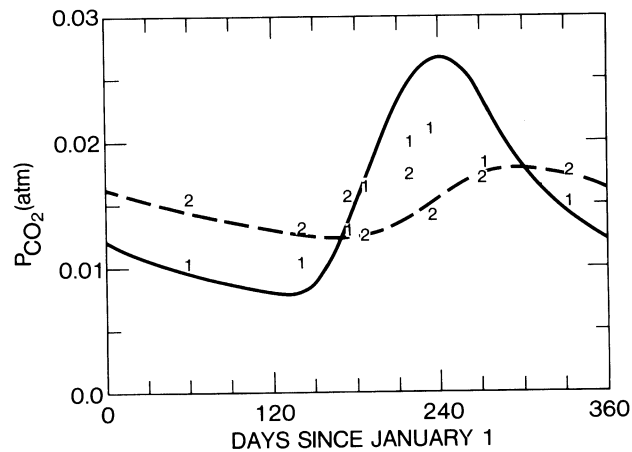


Fig 3. Comparison of calculated seasonal variation of P_{CO_2} at North Dakota Site 6 with observed data. Solid line: probe 1 model; dashed line: probe 2 model. Numbers are measured P_{CO_2} 's for probes 1 and 2, respectively. Probe 1 is screened at 3.0m, probe 2 at 5.8m.

agreement is quite good, indicating that diffusion theory adequately explains the Trout Creek data, even without incorporating site-specific parameters for their site.

The time variation of P_{CO_2} at the depths of probes 1 and 2, Site 6, from this simulation were also calculated and are compared with the measured values for Site 6 in figure 3. The comparison shows slightly less predicted seasonal variation for probe 1 than was observed; for probe 2, the predicted seasonal variation is somewhat greater than observed. Trial-and-error simulations (not shown) made by varying the tortuosity indicate that the amplitude and timing of the measured P_{CO_2} seasonal pattern for probe 1 can be very well simulated using a tortuosity of 0.07 ($\tau = 0.08$ is used in fig 3). Alternatively, an excellent match between measured and simulated results can be obtained for probe 2 using a tortuosity of 0.09. These tortuosities are both well within the plausible range for Site 6. However, an implausibly large value for tortuosity is required to force a simultaneous good fit to the data for both probes.

The inability to obtain a satisfactory simultaneous fit to the measured values for probes 1 and 2 at Site 6 suggests that the actual diffusion process may not be truly one-dimensional. A plausible explanation is that CO_2 moves by a somewhat less tortuous path from land surface to probe 2 than from land surface to probe 1, possibly due to a very local clay lens in the top three meters. However, the goodness of fit is adequate to strongly suggest that mainly vertical diffusion and calcite equilibrium are indeed the dominant mass-transport and mass-transfer mechanisms affecting the CO_2 distribution in the unsaturated zone at Site 6.

THE $^{14}CO_2$ MODEL. Boundary and initial conditions: The well-defined seasonal variation of $P_{^{14}CO_2}$ in the shallow probes

at Sites 6 and 4 (fig 4) suggests that diffusion is also important in the transport of $^{14}CO_2$. However, unlike CO_2 , atmospheric $P_{^{14}CO_2}$ has shown dramatic changes during the last

30 years as a result of atmospheric nuclear testing in the 1950's and 1960's. Because each species diffuses according to its own gradient, this post-bomb ^{14}C should have migrated at least tens of meters into the unsaturated zone by now. To test this idea, an attempt was made to simulate $P_{^{14}CO_2}$ at

Site 6, with the same media parameters used to simulate the seasonal effects described above.

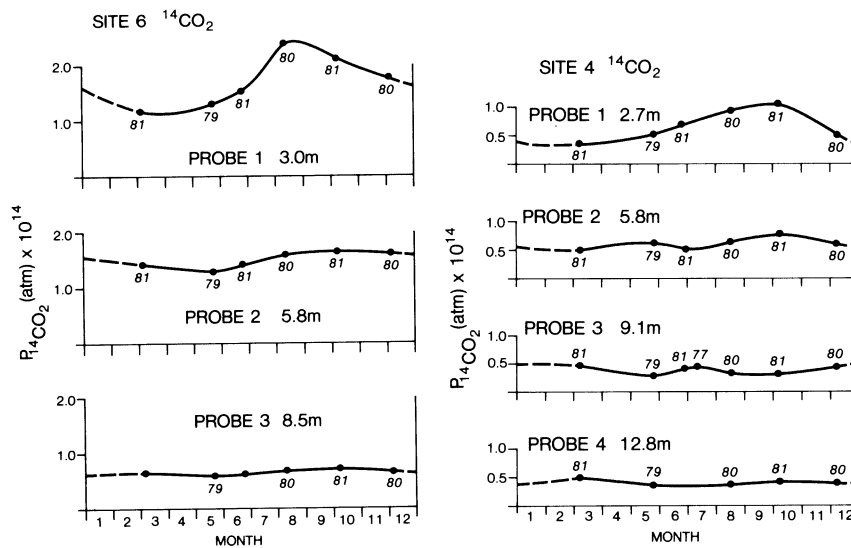


Fig 4. Seasonal variation of $P_{14}\text{CO}_2$ at North Dakota Sites 6 and 4. Data are plotted by collection date, independent of year, with the year of collection noted at each data point. Data from table 1.

To model $^{14}\text{CO}_2$, information is needed regarding the production of $^{14}\text{CO}_2$ in the root zone. $^{14}\text{CO}_2$ production was calculated from equation (34):

$$\bar{\alpha}_{14}\text{CO}_2(t) = [\bar{\alpha}_{14}\text{CO}_2(1981)] \times \frac{A^{14}\text{C}(t)}{A^{14}\text{C}(1981)} \quad (34)$$

where t = time;

$\bar{\alpha}_{14}\text{CO}_2(t)$ = average production rate of $^{14}\text{CO}_2$ in the root zone at time t , mol/cm³ of medium/sec;

and $A^{14}\text{C}(t)$ = activity (pmc) of ^{14}C in the atmosphere at time t (fig 5A).

The atmospheric ^{14}C activity through 1975 was estimated from data presented in figure 4 of Broecker, Peng, and Engh (1980),

and was then extrapolated to our measured values in 1981. $\alpha_{14}^{CO_2}$ (1981) was computed to produce an average $P_{14}^{CO_2}$ of 1.6×10^{-14} atm, the average Site 6 value measured at 3m. A 30-year period, starting in 1951, was simulated. Seasonal effects were ignored and 30-day time steps were used in the simulation. The proportionality postulated between atmospheric ^{14}C activity and soil-zone ^{14}C activity represents a major assumption that cannot be rigorously documented at present; the assumption is supported by the near-atmospheric ^{14}C activities in most of the surface CO_2 collections.

The mass transfer of $^{14}CO_2$ between the gas and liquid phases was also handled differently in this simulation. The ^{14}C mass transfer was assumed to occur at a rate proportional to that of CO_2^* . The soil gas was assumed to have an average partial pressure throughout the column of .014 atm. Using this value, the partitioning term in equation (32) reduces to $\{\theta_D + 1.10(\theta_T - \theta_D)\}$, thus linearizing equation (32) and making large time steps possible.

The lower boundary condition was also modified for this simulation. Diffusion in the liquid phase could be significant during the long time span covered; hence, another layer was added to represent the saturated material from 15m to 25m. As a mathematical artifice, these materials were assumed to have total and drained porosities of 0.35, and the tortuosity was assumed to be .0001. This approach allows gas diffusion through the fully-saturated medium to be approximated without reprogramming.

* This is not an obvious assumption. It is derived from a chemical model developed by the authors, the presentation of which is beyond the space limitations of this paper. The fundamental assumption is that dissolution and precipitation of calcite is governed by changes in P_{CO_2} .

This, in turn, leads to aqueous dilution or enrichment factors that overshadow the changes in $P_{14}^{CO_2}$.

Hence, the dependence on P_{CO_2} , rather than $P_{14}^{CO_2}$.

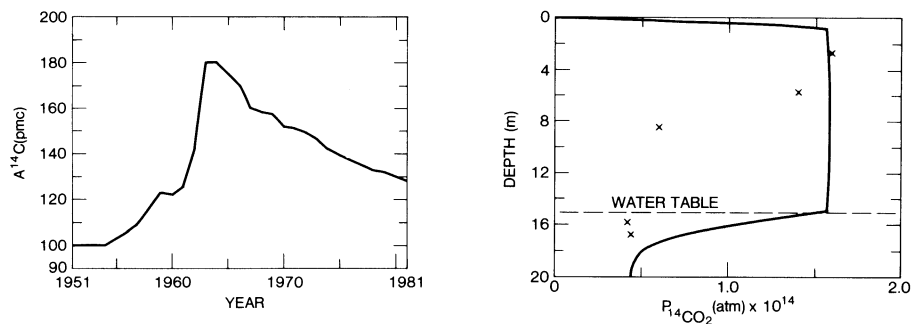


Fig 5. A. Atmospheric ^{14}C activity, adapted from Broecker, Peng, and Engh (1980); see text for discussion. B. Calculated depth profile for $P_{14}\text{CO}_2$ at North Dakota Site 6; see text for discussion.

Initial conditions to be assumed in the simulation of $^{14}\text{CO}_2$ are problematical, as the $^{14}\text{CO}_2$ profiles themselves suggest that they cannot be adequately explained by diffusion theory alone. For this simulation, it was assumed that $P_{14}\text{CO}_2$ in 1951 was equal to 0.48×10^{-14} atm, which is the same as that measured in the ground water in 1981.

RESULTS. The long-term ^{14}C simulation is shown in figure 5B. The calculated profile is almost vertical, with a slight bulge about mid-depth in the unsaturated zone arising from the effect of currently declining production rates following the 1964 peak in ^{14}C activity in the atmosphere. Note that the curve departs radically from the average measured partial pressures, symbolized by X's in the figure. The measured values show a sharp dropoff that cannot be explained by the gaseous diffusion-calcite equilibrium model. Moreover, according to theory, the dissolved $^{14}\text{CO}_2$ should have established a steep gradient to a depth of ca 3m into the water table during the 30-year period. The near equality of $^{14}\text{CO}_2$ partial pressures in the lower gas probes and groundwater samples at different depths (fig 6) shows that this has not been the case.

In spite of the clearly defined seasonal profile in the shallow probes (fig 4) application of diffusion theory to measured $^{14}\text{CO}_2$ profiles in the deep unsaturated zone indicates that some as yet unexplained mechanisms severely retard the migration of $^{14}\text{CO}_2$ with depth in the deep unsaturated zone. The general decreases in CO_2 and $^{14}\text{CO}_2$ cannot be readily explained with a steady state diffusion model because of the relatively large fluxes that can be achieved with gaseous diffusion. The depth distribution of CO_2 suggests transient processes on a fairly short time scale - not exceeding a few tens of years. The $^{14}\text{CO}_2$ is more rapidly attenuated with depth and shows a greater overall decrease than does CO_2 , suggesting a selective sink for $^{14}\text{CO}_2$ at Site 6. A time lag might also exist between changes in atmospheric ^{14}C activity and the ^{14}C activity in the root zone. However, if this were the only faulty assumption in the model, the decrease in $P_{^{14}\text{CO}_2}$ from 3m to 9m should not exceed ~30%, rather than the observed decrease of a factor of 2.

A particularly interesting observation is that soil gas-shallow groundwater $^{14}\text{CO}_2$ pressures approach equilibrium more closely than do the corresponding total P_{CO_2} 's, despite the selective attenuation of $^{14}\text{CO}_2$ with depth in the unsaturated zone at Site 6. No obvious processes to account for this phenomenon are apparent. However, whatever these mechanisms are, they can profoundly affect the ^{14}C activity of recharged ground water, and suggest that conclusions concerning the residence time of ground water in the unsaturated zone based solely on ^{14}C activities are extremely suspect.

An estimate of the relative magnitudes of diffusive and advective fluxes of CO_2 is needed. The following example, based on North Dakota Sites 4 and 6, provides a numerical comparison that might approximate Great Plains environments. Groundwater alkalinities in the area average ~10 meq/l; recharge in Bowman County is estimated as ~1 cm/yr (Croft, 1978). A recharge rate of 1ml $\text{H}_2\text{O}/\text{cm}^2\text{-yr}$ (ignoring media effects) yields a CO_2 flux to the water table of $10\mu\text{mol}/\text{cm}^2\text{-yr}$. In the gas phase a gradient of 1% CO_2 over 10m, including the moderating effects of porosity and reaction, provides a calculated diffusive flux of ~ $15\mu\text{mol}/\text{cm}^2\text{-yr}$. It thus appears that the diffusive fluxes due to the large, rapidly changing gradients associated with near-surface seasonal CO_2 fluctuations should overshadow recharge effects, while if smaller gradients occur in the deeper unsaturated zone the fluxes might approach each other in magnitude. Rough estimates suggest that sub-soil diffusion should pre-

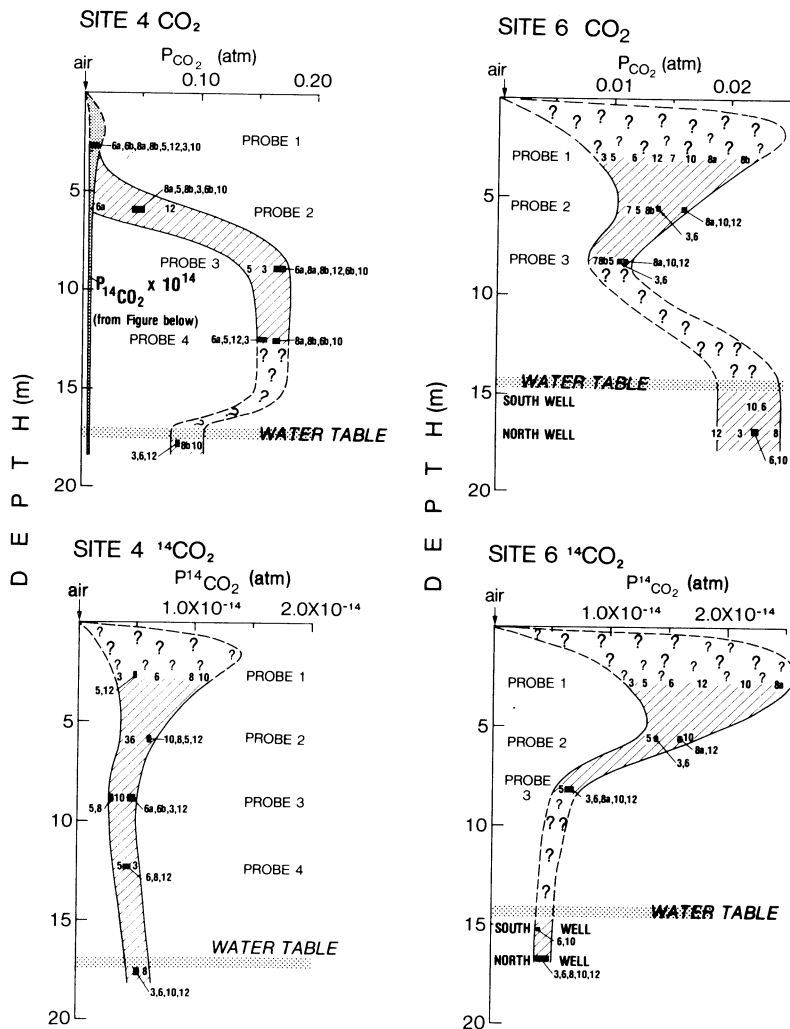


Fig 6. P_{CO_2} and $P^{14}\text{CO}_2$ vs depth at North Dakota Sites 4 and 6. Numbers refer to month of collection date, independent of year, and correspond to entries in table 1.

dominate for CO_2 and $^{14}\text{CO}_2$ at Sites 6, and CO_2 at Site 4; the relative magnitude of $^{14}\text{CO}_2$ diffusion below $\sim 5\text{m}$ at Site 4 is much less.

The data tables show that a wealth of information is available in the accumulated ^{13}C data for the unsaturated zone gases at all sites, both in terms of inter-site comparisons and in the differences between gases and the water table wells. No attempt has been made in this paper to incorporate these ^{13}C data into chemical models of unsaturated zone process. Also, no quantitative transport modeling for the other sites has yet been attempted. In the following discussion, important general aspects of the data at other sites are briefly pointed out.

DESCRIPTION OF OTHER SITES

NORTH DAKOTA SITE 4. (See Haas et al, 1983, for detailed description). This site provides an excellent example of the independent behavior of $^{12}\text{CO}_2$, $^{13}\text{CO}_2$, and $^{14}\text{CO}_2$. The major source of ^{12}C and ^{13}C in the system occurs at a depth of 7.5 to 9.5m, where oxidation in the upper portion of the lignite reduces oxygen pressure to near zero and produces CO_2 contents approaching 20 volume%. This CO_2 then diffuses upward, and masks the seasonal cycle in P_{CO_2} in all but the shallowest probe. The observed gradient in P_{CO_2} suggests that the CO_2 produced in this zone also diffuses downward towards the water table, which appears to be acting as a sink for CO_2 at this site.

In spite of P_{CO_2} -depth variation greater than an order of magnitude in the unsaturated zone, and three orders of magnitude difference relative to the atmosphere, the partial-pressure depth profiles of $^{14}\text{CO}_2$ are the most uniform observed in this study. The $^{14}\text{CO}_2$ depth profile is a better approximation to the elementary diffusion model (compare fig 6B with fig 1A) than either CO_2 or $^{13}\text{CO}_2$ from any other North Dakota sampling site. The surprising observation is again made that partial pressure equilibrium between the gas phase and the water table is approached more closely for $^{14}\text{CO}_2$ than for CO_2 . Note that here the partial pressure of CO_2 is lower in the water - opposite the situation present at North Dakota Site 6. The existence of the CO_2 gradient from the base of the lignite to the water table-if steady state-implies a large flux of $^{12}\text{CO}_2$ and $^{13}\text{CO}_2$ to the ground water.

NORTH DAKOTA SITES 2 AND 3. Both of these sites are located in lignite-rich spoils, and both show some of the general characteristics of North Dakota Site 4 - namely high and variable CO_2 contents due to lignite oxidation, and relatively uniform $^{14}\text{CO}_2$ profiles. Although an investigation of these sites was originally one of the motivations for this work, because of their hydrologic variability due to mine pumpage, we decided early to concentrate on natural processes in the undisturbed sites.

NORTH DAKOTA SITE 1. At Site 1 a stringer of lignite is present just above the water table and a perched water table (the gas probes pumped water) was present at depths of 3m to 8m until at least 1977. Prior to this, the deep samples at Site 1 resembled samples from similar depths at Site 4 in both CO_2 and $^{14}\text{CO}_2$ content. The perched water lens disappeared sometime between 1977 and 1980. From the latter date to the present the data at all depths show extreme variability; it was initially believed that the grouting had cracked or that some other sampling problem existed. However, more recent analysis of the data shows that the partial pressure of $^{14}\text{CO}_2$ is generally (not always) nearly constant, suggesting a lack of atmospheric influence. No plausible model for processes at this site is available at present.

THE TEXAS SITES. The sampling nests at both Texas sites were constructed as part of an artificial recharge study in the Ogallala aquifer conducted by the US Geological Survey (Weeks, 1978). At the Glenn and Lamb sites, located near Lubbock, Texas, the Ogallala formation consists of interbedded sands, silts, and clays, with local development of massive caliche. The water tables at the sites are at depths of 51m (Glenn) and 77m (Lamb). For additional geologic and hydrologic information, see Weeks (1978) and Petraitis (1981); much additional CO_2 and $\delta^{13}\text{C}$ data for these sites are presented in Petraitis (1981).

THE GLENN SITE. Two sets of samples were collected from this site (table 1). CO_2 partial pressures are 0.01 atm or less; highest CO_2 pressures occur at intermediate depths. In the single set of $^{14}\text{CO}_2$ samples collected, the relative variation of $P_{^{14}\text{CO}_2}$ is less than that of P_{CO_2} , but the greatest value is found at an intermediate depth. The partial pressure of $^{14}\text{CO}_2$ at this site is quite similar in magnitude to the values observed at North Dakota Site 4. No $^{14}\text{CO}_2$ data are available at the water table.

THE LAMB SITE. Two sets of CO_2 data are available, but in this case, they are quite dissimilar; only the shallow probes show fairly consistent values of P_{CO_2} . If the variation is

due to sampling error, it is most likely that the initial samples were collected without sufficient initial pumping.

This site is quite interesting in that it is the only site for which our data definitively show post-bomb $^{14}\text{CO}_2$ activities in deep samples, in spite of a perched water table at 28m. Combined with the relatively high CO_2 partial pressures, the resulting $^{14}\text{CO}_2$ partial pressures at the Lamb site are equalled only by the lignite spoils at North Dakota Site 3. The $^{14}\text{CO}_2$ partial pressures are nearly constant in the deeper probes.

GENERAL OBSERVATIONS

A number of general observations can be made regarding the behavior of $^{14}\text{CO}_2$ in the unsaturated zone that are independent of sampling location or date.

1) The geochemistry of $^{14}\text{CO}_2$ in the unsaturated zone must be evaluated in terms of both the partial pressure of $^{14}\text{CO}_2$ and the ^{14}C activity of the CO_2 gas samples. A value of $A^{14}\text{C} > 100\text{pmc}$ still remains the only unequivocal signature of post-bomb carbon. However, the general lack of correlation between the $A^{14}\text{C}$ and $P_{^{14}\text{CO}_2}$ depth profiles emphasizes the need for evaluation of both parameters in unsaturated zone ^{14}C studies.

2) Diffusion is a major mechanism of gas transport in the sub-soil unsaturated zone. The various isotopes of CO_2 each diffuse in response to their own sources and sinks, as best illustrated by the data from North Dakota Site 4. The diffusion models must consider individually the absolute concentration of each isotopic species in units of mass/volume or the corresponding gas partial pressures. Diffusive fluxes of CO_2 and its isotopes appear to predominate over advective fluxes in the shallow (< 5m) unsaturated zone. No generalizations regarding greater depths can be made.

3) $^{14}\text{CO}_2$ and $^{12}\text{CO}_2$ are biologically generated in the shallow soil zone. Penetration of the $^{14}\text{CO}_2$ into the unsaturated zone and observed activities $> 100\text{pmc}$ in surface samples imply relatively rapid diffusion of this species in the sub-surface. Considering the relatively large fluxes that can be generated by diffusive transport of gases, the variable

shapes of the P_{CO_2} - and $P_{^{14}\text{CO}_2}$ depth profiles and the partial pressure disequilibrium between the gas and aqueous phases suggest that steady-state processes are very unlikely at any of the sites studied.

4) The measured concentration, in mass/volume of gas, of $^{14}\text{CO}_2$ in the unsaturated zone is without exception 10 to 100 times greater than the concentration of $^{14}\text{CO}_2$ in the atmosphere.

ACKNOWLEDGMENTS

This has been a long and collective effort; however, some mention of individual areas of expertise seems warranted. DW Fisher was responsible for collection, analysis, and interpretation of the gas analyses; the very precise ^{14}C work is due to Herbert Haas; DC Thorstenson provided geochemical modeling concepts and ballast during field work in the high winds of the northern Great Plains; EP Weeks provided the transport modeling capability and the crucial initial observation that $^{14}\text{CO}_2$ must be dealt with in terms of partial pressures, and not simply in terms of ^{14}C activities. The manuscript was much improved as a result of discussion and review from Eric Sundquist and Ike Winograd. A number of people in the North Dakota District, Water Resources Division, US Geological Survey, willingly contributed many hours of help and support during the course of this project.

Finally, the existence of much of the data is due in large part to the continual good humor and competence--sometimes under extreme conditions--of Dave Stannard, whose help in the field is much appreciated.

REFERENCES

- Bavel, CHM van, 1951, A soil aeration theory based on diffusion: *Soil Sci*, v 72, p 33-46.
- Bird, RB, Stewart, WE, and Lightfoot, EN, 1960, *Transport phenomena*: New York, John Wiley and Sons, 780 p.
- Broecker, WS, Peng, T-H, and Engh, R, 1980, Modeling the carbon system, in Stuiver, M, and Kra, RS, eds, *Internatl ^{14}C Conf, 10th, Proc: Radiocarbon*, v 22, no. 3, p 565-598.
- Croft, MG, 1978, *Ground-water resources of Adams and Bowman Counties, North Dakota*: North Dakota Geol Survey Bull, 165 (III), 54 p.

- Feynman, RP, Leighton, RB, and Sands, M, 1963, The Feynman lectures on physics, vol 1, chap 43: Reading, Mass, Addison-Wesley Pub Co, Inc.
- Garrels, RM and Christ, CL, 1965, Solutions, minerals, and equilibria: New York, Harper & Row, 450 p.
- Haas, H, Fisher, DW, Thorstenson, DC, and Weeks, EP, 1983, ^{13}C and ^{14}C measurements on soil atmosphere sampled in the sub-surface unsaturated zone in the western great plains of the US: Radiocarbon, v 25.
- Jost, W, 1960, Diffusion in solids, liquids, gases: New York, Academic Press, 3rd printing with addendum, 652 p.
- Kunkler, JL, 1969, The sources of carbon dioxide in the zone of aeration of the Bandelier Tuff, near Los Alamos, New Mexico: US Geol Survey Prof Paper 650-13, p B185-B188.
- Lai, S-H, Tiedje, JM, and Erickson, AE, 1976, In situ measurement of gas diffusion coefficient in soil: Soil Sci Soc America, v 40, no. 1, p 3-6.
- Landergren, S, 1954, On the relative abundance of the stable carbon isotopes in marine sediments: Deep Sea Research, v 1, p 98-120.
- Li, YH, and Gregory, S, 1974, Diffusion of ions in sea water and in deep-sea sediments: Geochim et Cosmochim Acta, v 38, p 703-714.
- Petratis, MJ, 1981, Carbon dioxide in the unsaturated zone of the southern high plains of Texas: Unpublished master's thesis, Lubbock, Texas, Texas Tech Univ, 134 p.
- Plummer, LN, and Busenberg, E, 1982, The solubilities of calcite, aragonite, and vaterite in $\text{CO}_2\text{-H}_2\text{O}$ solutions between 0 and 90°C, and an evaluation of the aqueous model for the system $\text{CaCO}_3\text{-CO}_2\text{-H}_2\text{O}$: Geochim et Cosmochim Acta, v 46, p 1011-1040.
- Reardon, EJ, Allison, GB, and Fritz, P, 1979, Seasonal chemical and isotopic variations of soil CO_2 at Trout Creek, Ontario: Jour Hydrology, v 43, p 355-371.
- Reardon, EJ, Mozeto, AA, and Fritz, P, 1980, Recharge in northern climate calcareous sandy soils: soil water chemical and carbon-14 evolution: Geochim et Cosmochim Acta, v 44, p 1723-1735.
- Weeks, EP, 1978, Field determination of vertical permeability to air in the unsaturated zone: US Geol Survey Prof Paper 1057, 41 p.
- Weeks, EP, Earp, DE, and Thompson, GM, 1982, Use of atmospheric fluorocarbons F-11 and F-12 to determine the diffusion parameters of the unsaturated zone in the southern High Plains of Texas: Water Resources Research, in press.